Liquid Crystals
Publication details, including instructions for authors and subscription information:
http://www.informaworld.com/smpp/title~content=t713926090

Electroconvective flow propagation and defect formation in MBBA

K. S. Krishnamurthy[a]; R. Balakrishnan[a]
[a] Faculty of Electrical and Mechanical Engineering, College of Military Engineering, Pune, India

To cite this Article Krishnamurthy, K. S. and Balakrishnan, R.(1994) 'Electroconvective flow propagation and defect formation in MBBA', Liquid Crystals, 16: 3, 413 — 420
To link to this Article: DOI: 10.1080/02678299408029166
URL: http://dx.doi.org/10.1080/02678299408029166

LIQUID CRYSTALS, 1994, VOL. 16, NO. 3, 413–420

Electroconvective flow propagation and defect formation in MBBA

by K. S. KRISHNAMURTHY* and R. BALAKRISHNAN
Faculty of Electrical and Mechanical Engineering,
College of Military Engineering, Pune 411 031, India

(*Received 6 November 1992; accepted 23 July 1993*)

A new type of highly organized, large scale propagation of vortical flow has been observed in MBBA subject to a transverse electric field. This is a transient phenomenon associated with the transformation, occurring at elevated voltages, between electrically distorted homeotropic and planar states. The convective flows generate an array of linear defects which persist even after removal of the field.

1. Introduction

Nematic liquid crystals with a negative dielectric anisotropy and positive conductivity anisotropy are known to display a rich variety of electroconvective phenomena under varying conditions of excitation [1]. Studies on the evolution of turbulence have shown that, generally, the roll structure into which a suitably aligned nematic bifurcates at the threshold, passes progressively through several prechaotic secondary instabilities, as the driving field is increased [2–4]. However, so far, there appears to have been no reported instance of an electrohydrodynamic state undergoing a major structural transition on the route to chaos. We have observed such a heterogeneous change of structure in the conduction regime of MBBA (4-methoxybenzylidene-4′-*n*-butylaniline), and it is the purpose here to describe the fascinating novel aspects of this phenomenon.

2. Experimental

The nematic material MBBA was studied at room temperature (30°C), using the transverse geometry shown in figure 1 (*a*). The sample thickness z was $\sim 75\,\mu$m and the length x, $\sim 1{\cdot}5$ cm; the width y, or the electrode separation, was varied in the range 300–1400 μm. The field frequency was 50 Hz. The observations were made along the Z direction, in transmitted mercury light, using a Leitz polarizing microscope. For interference experiments, a green filter was used, and the transmission axes of the polarizer P and analyser A were set either along X and Y (axial position) or at 45° to X and Y (diagonal position). Figure 1 (*b*) shows the director pattern in the rest state. The nematic fluid was introduced into the cell cavity from one end using capillary action. At first, the flow-induced alignment was homogeneous (H) along X; but the molecules reoriented spontaneously over a period of several minutes to result in a $-1/2$ singular line near the lateral boundaries and homeotropic (V) alignment everywhere else. The existence of splay-bend deformations close to the electrode edges was inferred from observations on the peripheral birefringence bands using a Berek compensator.

*Author for correspondence.

0267–8292/94 $10·00

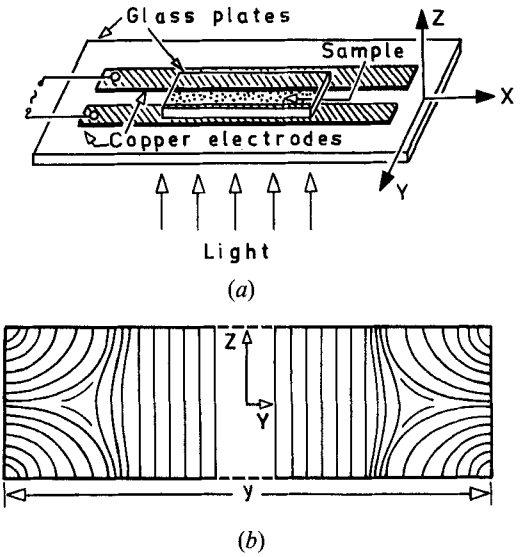

Figure 1. (*a*) Experimental arrangement for observing the electroconvective effects. (*b*) The initial director field.

3. Results and discussion

The sample subjected to a gradually increasing field undergoes the first bifurcation to what may be described as the distorted homeotropic state V_D, at a well-defined threshold V_{th}. Figure 2(*a*) presents the V_D texture at $\sim 1{\cdot}15\,V_{th}$, for crossed polarizers in the diagonal position. For a given elliptical fringe system here, the order of interference is the highest at the centre C, from where the distortion evolves. Further, the domains of elliptical fringes become nearly extinct when the polarizers are set in the axial position (see figure 2(*b*)). Thus the closed fringes in figure 2(*a*) arise due to molecular tilts in the *YZ*-plane and these tilts take place in opposite directions for adjacent domains. This is further confirmed by the focal power which the elliptical domains possess for light vibrating along *Y*; the power vanishes when the vibration is along *X*. However, the boundary regions B on either side of the interdomain junctions O exhibit lens action for light vibrating along *X*; also, birefringence fringes are seen in these regions when the polarizers are in the axial position (see figures 2(*b*) and (*c*)). All these observations lead to the director configuration shown in figure 3 for the V_D state near its threshold.

Most of these features of the V_D state are long since known [5–8]. However, regarding the hydrodynamic flows in this state, there appears to be some confusion. We find that the tracer particles revolve in the *XY*-plane, and not in the *YZ*-plane as earlier reported [7]. The flow lines, which are nearly elliptical, go round the interdomain junctions O rather than the domain centres C. Significantly, unlike the situation for a Williams domain instability in sandwich cells [1], the molecular tilt varies continuously along these lines.

Figure 2(*c*) shows the complex nature of the V_D state at elevated voltages. While at O the molecules still remain vertical, on either side of O, the B regions exhibit new fringe systems. Their visibility is a maximum for the axial setting of the crossed polarizers, but a minimum for the diagonal setting. Further the B regions become

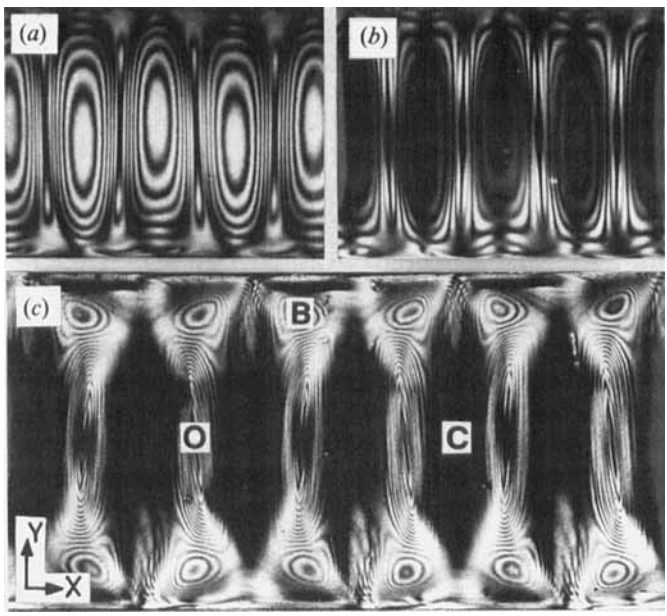

Figure 2. Textures of the distorted homeotropic state in MBBA; 720 μm wide sample; 50 Hz. (*a*) Crossed polarizers in the 45° position, 65 V_{rms}. (*b*) Same region as in (*a*), crossed polarizers along X and Y, 65 V_{rms}. (*c*) Crossed polarizers along X and Y, 76 V_{rms}.

nearly extinct for parallel polarizers in the 45° position. Clearly these zones are optically active, with the structure twisted about Z. The twists are of opposite sign for adjacent zones along X and the same sign for opposite zones along Y. Furthermore, the rope-like fringe pattern in the mid-region seems to indicate a structural torsion about Y. The director field responsible for the pattern in figure 2(*c*) remains to be understood.

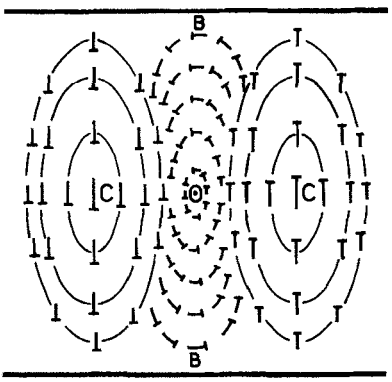

Figure 3. Director pattern corresponding to the distorted homeotropic state near the instability threshold.

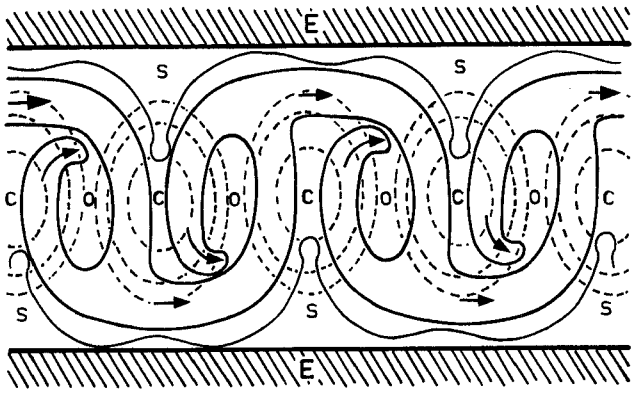

Figure 4. Representation of the mode of convective propagation characterizing the transition between distorted homeotropic and planar states in MBBA.

When the convective structure reaches the complexity indicated in figure 2(*c*), the V_D state becomes unstable. Transformation to a distorted planar state H_D follows. The onset of H_D is without a definite threshold; though unpredictable in time, it generally occurs sooner at higher fields when the fluid motion in the V_D state is intense (but not turbulent). The growth of the H_D structure involves nucleation. Very often, the transition originates near the end free-surfaces or around air-pockets, where facile molecular reorientation is possible. Its future course is very predictable, being determined by the nature of cellular flows already present in the V_D state. In figure 4 showing the propagation, the dotted elliptical lines represent the fringes in the V_D state for the diagonal setting of the polarizers. The H_D fluid, contained between the pair of thick lines in the figure, flows in from the left. It curls around the first of the junctions O, clockwise; just as the first cycle is completed, the vortex extends from the lower right to circulate anti-clockwise around the next junction O. The process repeats until all the specimen is in the H_D state. After the first circulation around a given junction, subsequent cycles are seen as a closing in of the H_D fluid, and eventually the vortex axis at O remains a linear defect in the new state. A part of the fluid near the electrodes which gets dragged by the convective current, peels off it, and recedes to remain in the original state. This *stagnant* part S lies between the thin lines and electrode edges in figure 4.

The textures in figure 5 depict the H_D growth pattern. During the flow, as may be seen in figures 5(*h*) and 5(*i*), the ovals of circulation are obliquely oriented, with their inclinations in opposite directions for adjacent vortices. Also, after the establishment of the H_D state, the dust particles revolve in tilted ellipses around O. A similar flow pattern is also present for freely suspended nematic layers [9], where it has been ascribed to variations in sample thickness. Evidently, for our *bound* samples, this explanation is not valid. Moreover, the vortex mode in freely suspended layers is essentially the *isotropic mode*, whereas with the specimens here, the circulation ceases above the clearing point. It is possible that the obliquity of flow paths arises from differences in certain elastic moduli and is associated with the non-linear *squint* term in hydrodynamic equations, as in the case of the Williams domain mode [10]. Another significant aspect of the H_D texture observed with crossed polarizers in the diagonal position concerns the nearly triangular fringes (see

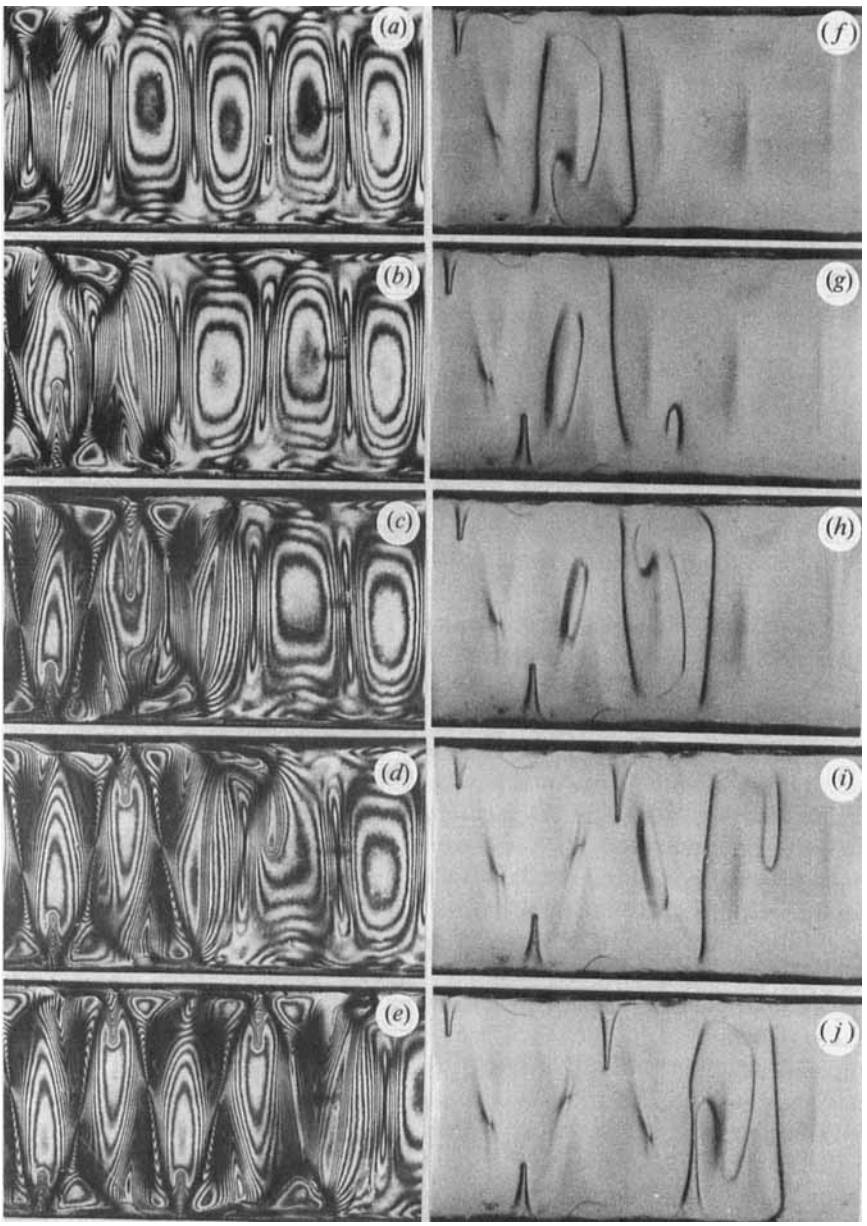

Figure 5. Time evolution of the distorted planar structure, from the distorted homeotropic state, showing an organized propagative transition. For (*a*)-(*e*), crossed polarizers in the 45° position, electrodes 720 μm apart. For (*f*)-(*j*), only analyser along the field direction *Y*, electrodes 677 μm apart. After inducing the transition at $\sim 72\ V_{rms}$, voltage lowered to $\sim 58\ V_{rms}$ to slow down the flow for ease of recording.

figure 5 (*e*)) formed in place of the earlier elliptical fringes (see figure 2 (*a*)). The order of these fringes, unlike that of the elliptical fringes, increases from the centre outwards. In other words, the out-of-layer molecular tilt becomes progressively less from the centre outwards, as is apt to be the case with a distorted planar structure.

We propose to discuss the quantitative aspects of the propagation just described elsewhere. The main results are briefly the following: for a 70 μm wide sample, the average speed v_x (in $\mu m\,s^{-1}$) of propagation along X varies with voltage (for the range 48 to 90 V_{rms}) according to $v_x = 0{\cdot}21\,V_{rms} - 8{\cdot}0$; the average speed v_y in the mid-region varies non-linearly with voltage, between 15 $\mu m\,s^{-1}$ at 45 V_{rms} and 90 $\mu m\,s^{-1}$ at 80 V_{rms}; v_y (in $\mu m\,s^{-1}$) decreases linearly with an increase in y (between 80 μm and 1100 μm), being given by $v_y = 106 - 0{\cdot}088y$, for $V_{rms} = 70$ V, and for the type of flow in figure 4; the rate of change of v_y with y seems to depend on the type of vortex, for a second linear region appears in the v_y-y plot corresponding to faster flows at which the vortical stream starts breaking.

While the H_D fluid is propagating, if the voltage is decreased to slightly lower than V_{th}, still the propagation continues, albeit very slowly, but the mode of flow is sinusoidal between the electrodes. On the contrary, if the voltage is increased (or y is decreased) to drive the fluid into rapid convection or swirling, the H_D stream breaks into islands in the mid-region. Yet each island follows the original vortex line. During the V_D-H_D transformation, if the voltage is momentarily increased to obtain turbulence and then decreased, the original pattern of the H_D region, as well as the initial growth pattern of H_D, is recovered. If the turbulence is prolonged, this recovery is absent; then linear defects of strength $+1$ and -1 appear randomly. As noted by Chang [6], turbulence seems to involve a random shift of vortex centres or defects.

Interestingly vortical flow propagation in non-uniformly thick, freely suspended smectic films seems to resemble that in figure 5 [11]. However, for nematics, this type of nucleated and regular growth behaviour has not been reported earlier. We may emphasize that the propagative phenomenon observed here is a transient one, characterizing the mode of alignment transition; it is obviously different from the sustained translatory instability of the Williams domains reported in [12]. While the mechanism responsible for the flows observed by us remains to be understood, the alignment transition itself may be related to the anchoring conditions existing at the metal and glass walls. As previously mentioned with reference to figure 1 (*b*), the sample was initially homogeneous due to capillary flow. But a strong tendency of the molecules to lie along Y at the metal-nematic interface forced a $-1/2$ disclination to develop near the electrode edges. Then, presumably because of a weak anchoring at the glass-nematic interface, the V-H boundaries near the electrodes moved in and disappeared in time to give a bulk homeotropic state. Not surprisingly, therefore, when the electric field distorts the specimen so formed to an extent that the H_D structure becomes energetically more favourable than the V_D structure, the transition to the H_D state follows.

The V_D-H_D transition is not directly reversible by reducing the field strength. On turning the field off, the H_D state changes to a degenerate H state which is metastable; it reverts to the V state by a gradual collapse of the H region in lateral directions. Figure 6 shows an H zone between two V zones. The V-H boundary along X is a twist wall. The boundary has periodic cusp-like regions where modified $-1/2$ singular lines are located. In the mid-region is seen a fascinating array of $+1$ linear defects which are connected to the $-1/2$ disclinations along the boundaries.

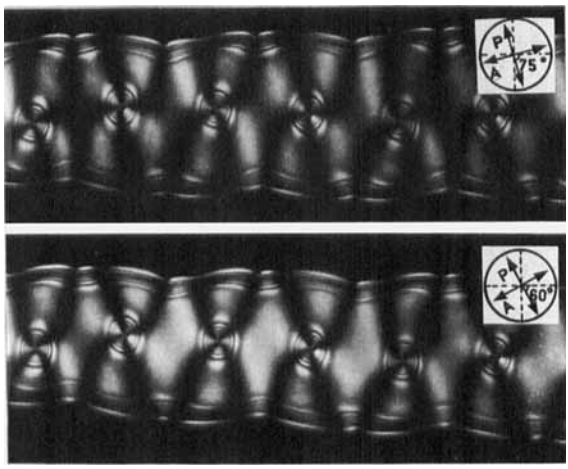

Figure 6. An array of +1 linear defects within the planar structure of MBBA, connected to modified −1/2 disclinations at the boundaries. Field-off state. Crossed polarizers, rotated counterclockwise from (*a*) to (*b*). Homeotropic dark regions to either side of the planar domain, gradually extending into the domain.

The molecular arrangement around the +1 defects is essentially tangential as found using a Berek compensator. The circular fringes around this defect are due to tilting of the molecules in vertical planes. The director field corresponding to the H texture is provided in figure 7.

We are grateful to the Commandant, College of Military Engineering, for the experimental facilities.

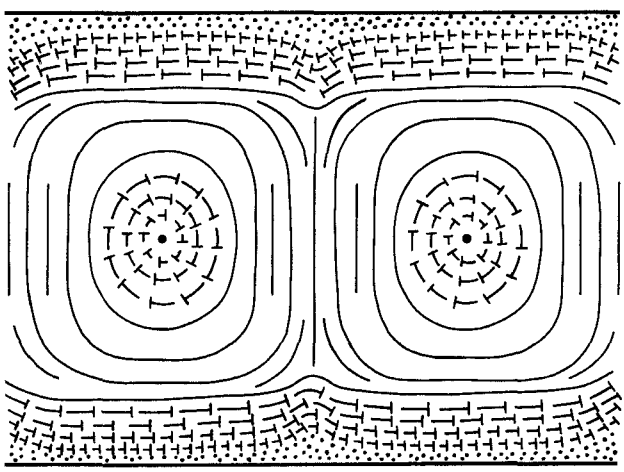

Figure 7. Director pattern for the metastable planar state with regularly formed +1 and −1/2 defects.

References

[1] BLINOV, L. M., 1983, *Electro-Optical and Magneto-Optical Properties of Liquid Crystals* (Wiley).
[2] HIRAKAWA, K., and KAI, S., 1977, *Molec. Crystals liq. Crystals*, **40,** 261.
[3] RIBOTTA, R., 1992, *Solitons in Liquid Crystals*, edited by L. Lam and J. Prost (Springer-Verlag), p. 264.
[4] DELEV, V. A., SCALDIN, O. A., and CHUVYROV, A. N., 1992, *Liq. Crystals*, **12,** 441.
[5] FREEDERICKSZ, V., and ZOLINA, V., 1933, *Trans. Faraday Soc.*, **29,** 919.
[6] CHANG, R., 1973, *Molec. Crystals liq. Crystals*, **44,** 1885.
[7] KARAT, P. P., and MADHUSUDANA, N. V., 1975, *Pramana*, Suppl. No. **1,** p. 285.
[8] FAETTI, S., FRONZONI, L., and ROLLA, P. A., 1983, *J. chem. Phys.*, **79,** 1427.
[9] FAETTI, S., FRONZONI, L., and ROLLA, P. A., 1983, *J. chem. Phys.*, **79,** 5054.
[10] BEN-ABRAHAM, S. I., 1979, *J. Phys. Colloque, Paris*, **40,** C-3-259.
[11] MORRIS, S. W., 1992, *Liq. Crystals Today*, **2,** 4; MORRIS, S. W., DE BRUYN, J. R., and MAY, A. D., 1991, *J. statist. Phys.*, **64,** 1021.
[12] JOETS, A., and RIBOTTA, R., 1989, *Liq. Crystals*, **5,** 717; 1988, *Phys. Rev. Lett.*, **60,** 2164; REHBERG, I., RASENA, S., and STEINBERG, V., 1989, *Phys. Rev. Lett.*, **62,** 756.